Wilmer A. Pardo[1,3]
Mònica Mir[1,2]
Josep Samitier[1,2,3]

[1]Nanobioengineering Laboratory, Institute for Bioengineering of Catalonia (IBEC), Barcelona, Spain
[2]The Biomedical Research Networking Center in Bioengineering, Biomaterials and Nanomedicine (CIBER-BBN), Zaragoza, Spain
[3]Department of Electronics, University of Barcelona (UB), Barcelona, Spain

Received January 30, 2015
Revised April 29, 2015
Accepted April 29, 2015

Research Article

Signal enhancement in ultraflat electrochemical DNA biosensors

The ability of holding back the undesired molecules, but at the same time to provide the right distribution and orientation of the bioreceptors, are critical targets to reach an efficient hybridization and enhanced detection in electrochemical DNA biosensors. The main actors responsible of these key functions are the substrate of the sensor and the interface auto-assembled on it. In this paper we present the annealing as a method to improve commercial gold evaporated substrates for biosensor applications. The restructuring of granulated gold surface by means of annealing heating treatment leads to the formation of ultraflat gold lamellar terraces. The formation of terraces was characterized with scanning tunneling microscopy and optical interferometry. The performance of the sensor sensitivity on granular substrates and ultraflat substrates was studied, concerning the orientation and surface coverage of the bioreceptor interface applied in electrochemical biosensor. The hybridization efficiency of ferrocene-labeled DNA amplified by PCR was characterized with surface plasmon resonance and electrochemistry. The experimental results demonstrate that annealing process, positive influence on optical and voltammetric readings, due to a structured organization of the bioreceptors on the flat substrate, gaining more efficient immobilization and DNA hybridization. The results suggest the annealing as a powerful tool for improving gold substrates in biosensors applications.

Keywords:
Annealing ultraflat surfaces / DNA biosensor / DNA hybridization / Electrochemistry / Self-assembled monolayer
DOI 10.1002/elps.201500049

1 Introduction

Chemisorption of thiolated molecules chains on gold leads to well-structured self-assembled monolayers (SAMs). SAMs are ordered molecular assemblies formed by a strong and spontaneous chemical bond and weak intermolecular interactions between its components on a solid support. This assembly is given by the adsorption of a molecular constituent (called head group, usually a thiol molecule) on a gold substrate. Self-assembly at the nanoscale is itself a purely molecular process that requires a wide network of connections and full interactivity between them. In the self-assembly process there are several topics to consider, including the type of assembly and the nature of the interface [1]. SAMs on metal surfaces have attracted considerable attention because to their importance in fundamental bioresearch and also in technological applications such as electronic devices and chemistry supramolecular assemblies applications. SAMs offer a versatile platform for nanotechnology being widely used in electrochemical and optical biosensors [2, 3]

Biosensors are devices that include a complex, highly specific, and sensitive biodetection process. These features cause the most common problems on developing efficient sensor devices [4–6]. The affinity between complementary bioelements that are chosen as analytes and receptors is crucial. So, relation between structures such as antigen-antibody, receptor-hormone, or DNA capture probe-complementary target are of great importance. But not only the affinity constant between the two main actors is responsible of a productive interaction, also the orientation of the bioreceptor on the sensor surface plays a key role in the interaction.

The ideal conception of a biosensor consists on the reproduction of molecular biological interactions on inorganic platforms. This bioreactions are detected by physicochemical transduction. The most common transducers for biosensors applications are based on optical techniques such as surface plasmon resonance (SPR), fluorescence, among others [7]. However, electrochemical detection offers a low cost biosensor production, portability, and sensitivity [8]. For electrochemical DNA biosensors, a good distribution of the biomolecules on the solid substrates, mainly on gold electrodes, provides less obstruction for the bioreceptor and the analyte interaction. The electron transfer from the label to

Correspondence: Dr. Mònica Mir, Nanobioengineering Laboratory, Institute for Bioengineering of Catalonia (IBEC), Baldiri Reixac, 10–12, Barcelona, Spain
E-mail: mmir@ibecbarcelona.eu

Abbreviations: **DPV**, differential pulse voltammetry; **SAM**, self-assembled monolayer; **SPR**, surface plasmon resonance; **STM**, scanning tunneling microscopy

Colour Online: See the article online to view Figs. 1, 2, and 4 in colour.

the electrode, the hybridization efficiency, and the quality of the detection signal are beneficiated after the optimization of the anchor patterned [9, 10].

Besides the way for capture probe immobilization, the surface substrates play a key role on the distribution of the bioreceptors on the surface. The most conventional methods of gold chips fabrication for biosensors applications are based on sputtering and evaporation of gold on a glass surface [11, 12] However, the high roughness of these substrates is not appropriate for an optimum pattern and so; the organization of the recognition bioelements is affected [13]. Besides, the formation of gold islands on the deposited layer, condition the effectiveness, and sensitivity of biosensor [14].

Ultraflat surface are essentials in wherein the nanometric characterizations of the surface patterns is required, such as: bond distances, atomic distances, molecular orientation, single molecule conductance, among others [15–17]. Generally gold evaporated mica surface are used for this purpose, but the fragility of this material difficult its application. In a more robust way, gold evaporate glass substrates with an annealing posttreatment are used in the same applications. Ultraflat annealing consists on heating the gold particles above its critical temperature, altering the microstructure of this material, to obtain a better rearrangement of their crystallographic characteristics and to reduce the surface roughness [18, 19]. However, these kinds of ultraflat substrates have never used in practical biosensors applications. So, the impact of this posttreatment on the hybridization efficiency and the quality of the electrochemical signal in DNA biosensors has not studied or reported in literature.

In this work, the annealing is presented as a treatment to modify commercial gold surfaces and used as platforms for DNA electrochemical biosensors. The effect of the annealing on gold substrates has been characterized with scanning tunneling microscopy (STM) and optical interferometry. SPR and electrochemical techniques have been used to characterize the monolayer distribution of the bioreceptors and to measure the target hybridization efficiency on the two studied substrates, annealed and untreated gold substrates. The DNA sample analyzed is a real amplified PCR DNA sample specific for prostate cancer.

2 Materials and methods

2.1 Material and chemicals

Maleimide-polyethylene glycol disulfide (MalPEG) -HO-EG6-C11-S-S-C11-EG6-NHCO-Maleimide- was supplied by ProChimia. 6-Mercapto-1-hexanol (MCH), Tris-HCl, EDTA, magnesium chloride ($MgCl_2$), sodic phosphate (Na_2HPO_4), triton, sodium citrate, potassium chloride (KCl), potassium dihydrogen phosphate (KH_2PO_4), and sodium chloride (NaCl) were purchased from Sigma. All aqueous solutions were prepared in double distilled MilliQ water. The DNA was manufactured by Metabion International AG. The complementary capture probe sequence was 3' SH-CGTGTTTGTCCGCTTTCGTGGTC 5' and the noncomplementary capture probe sequence was 3' SH-GGCAAAGCGCAGGGTCT 5'. The DNA target complementary was amplified by PCR with Qiagen PCR reagents. The amplified target DNA had a size of 106 mer; 3'GCCCAGTAGATGCCCCTGTGCCTGTC**GCACAAACAGGCGAAAGCACCYG**ACTGCGGCGTCCGAGACCACCGCGCACCCGGGTCGGACCGCGTGATGCACTGCCGAA '5, the region where the capture probe hybridizes is marked in bold. The amplification was performed with a ferrocene labeled primer, generating a target ferrocene labeled at 5' end.

2.2 Annealing treatment

The gold substrates purchased from Menzel–Gläser consist in BK7 glass square chips of 2 cm^2 with refraction index (n) 1.5151 and coated with 2 nm of chromium and 50 nm of gold, which were deposited by evaporation with an Edwards Auto 306 evaporator. For its cleaning, first it was sonicated in ethanol for 5 min and then it was dried with nitrogen. Finally, the chip was placed in UV for 10 min. For the annealing treatment, it was used a butane flame for 5 min at a distance of 3 cm from the chip, making a zigzag movement onto gold surface. The chips were cooled under argon atmosphere at room temperature.

2.3 STM and optical interferometry

To characterize the structural changes given by annealing on the gold surface both STM experiments and interferometry were performed. To obtain roughness and waviness values a Veeco STM Agilent and Optical Interferometer Veeco Wyko 9300 NT were used respectively. The measurements were performed in air in both cases.

2.4 DNA target amplification by PCR

The PCR amplification of the DNA template was performed with 10^6 target DNA molecules. It was used a standard amplification protocol from Quiagen, where is included; H_2O RNAse free, dNTPs 10 mM each one, buffer enzyme, Q solution, and RT one step enzyme and internal control oligonucleotide. For starting reaction, we assembled all reagents on ice, adding polymerase enzyme last. This mixture is transferred to the thermocycler preheated to denaturation temperature (95°C) for 15 min. The PCR cycles used were: 30 amplification cycles of 95ºC (0.5 min), 56ºC (1.5 min), and 72ºC (1 min) was performed. Later, one cycle at 72ºC for 10 min was performed to end the DNA polymerization. Finally the thermocycler is kept under 4ºC until the tubes are collected.

2.5 Functionalization of gold surface. SPR and electrochemical biosensor characterization: Bioreceptors immobilization

The gold chips were cleaned as was described in the annealing treatment protocol and annealed or untreated the gold substrate. Then the substrates were functionalized with specific thiolated DNA capture probes. This immobilization was performed by immersing for two hours in 20 μM solution of MalPEG diluted in 10 mM Tris-HCL, 1mM EDTA, 5 mM $MgCl_2$, and 1 M NaCl at pH 7.5 (Tris Buffer), and then incubated inside 10 μM solution of CP diluted in tris buffer for one hour. Once the CP was immobilize. In order to block free Maleimide groups from the linkers, the chips was incubated for one hour in 20 μM solution of MCH diluted in Tris buffer. The oligonucleotide target used for this detection was amplified by PCR, obtaining a 110 mer ferrocene labeled dsDNA, as was detailed before. The amplified target was not separated from the PCR reagents and so a complex matrix of enzyme, ferrocene labeled primer and remaining DNA are inside the target solution. The amplified dsDNA was denatured at 90ºC for 10 min and then kept into ice. For the hybridization of the target, the amplified sample was diluted (1:20) with 250 mM NaH_2PO_4, 15 mM Sodium citrate, 150 mM NaCl, 1 mM EDTA, and 0,02 mM Triton at pH 7,4 (hybridization buffer) and incubated on the CP functionalized chip for 1 h. All immobilizations were performed at room temperature in the electrochemical SPR chamber at flow rate of 300 μL/min. Between each immobilization steps the chips was rinsed with 1 M NaCl, 1mM KCl, 1 mM Na_2HPO_4, and 1 mM KH_2PO_4 (washing buffer).

Before and after each immobilization step, it was made a scan to determine the angle shift due to the biomolecule immobilization on the SPR chip. The reflected intensity is monitored as a function of the incidence angle, which gives the angular reflectivity. The SPR angle shifts were converted into mass uptakes surface coverage Γ, using the experimentally determined relationship reported in the literature [20,21]. SPR was performed under Kretschmann configuration with a custom-made setup from Res-Tec Company (Germany).

Electrochemical measurements were performed in 10 mM NaCl by differential pulse voltammetry (DPV). For this purpose CH660C potentiostat from CH Instruments was used.

3 Results and discussion

The gold BK7 glass substrates commonly used in SPR and electrochemical biosensors are fabricated by the evaporation of gold in a vacuum chamber where the glass substrates are deposited by condensed atoms of gold. This is a common method for thin film deposition, but the obtained surfaces have pebble-type structures with high roughness and contain gold islands. The annealing treatment on these substrates restructures the crystallographic organization of gold, leading to formation of flat terraces with a pronounced (111) texture.

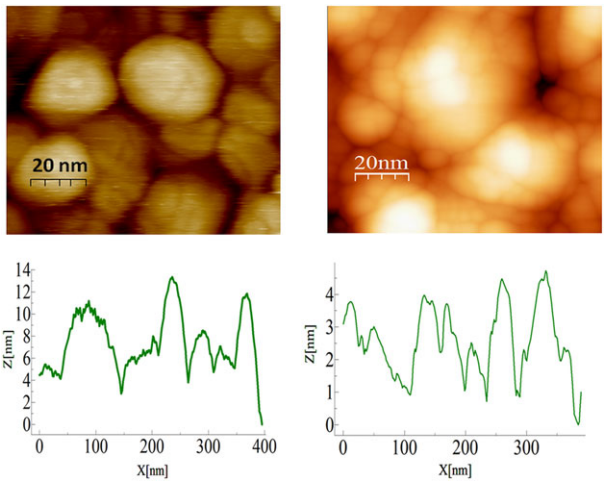

Figure 1. STM images taken on the nonannealed (left side) and annealed gold substrates (right side). Bottom graphs show the section profile along a line drawn on both substrates.

Annealing is a widespread method to obtain ultraflat surfaces for nanometric characterizations methods. This transition is temperature dependent [22], and influenced by the distance between the flame and the gold surface and the heating time [23]. It is reported that the gold layer thickness also influences the quality of the new flat terraces [24].

3.1 STM substrate characterization

The typical gold evaporated SPR chips are no truly flat. A quick look on the STM characterization (Fig. 1) reveals the differences in shape, size, and the condition of the gold grains before (left) and after (right) surface heating treatment. The fusion of the gold islands found on the unannealed substrates, generates after heating grain enlargement organized as flat terraces, giving homogeneity to the surface nanostructure. The gold grain size average in the pebble-type untreated substrate is 14 nm, while it is reduced to 4 nm after the gold restructuration by the annealing process, reducing the surface roughness of the substrate.

3.2 Optical interferometry substrate characterization

Nanoscale characterization blinds us to another important surface characteristic; the waviness. It is a broader view of roughness and its measurement permits to observe irregularities more periodic, whose spacing is greater than the roughness length.

The roughness and waviness of gold surface does not depend exclusively on the method in which is deposited the metal on the substrate, but also strongly depends on the nature of the solid support. Often it is believed that the supports are stable solids. However, high temperatures and frequent shelling during the processes of gold deposition have effects

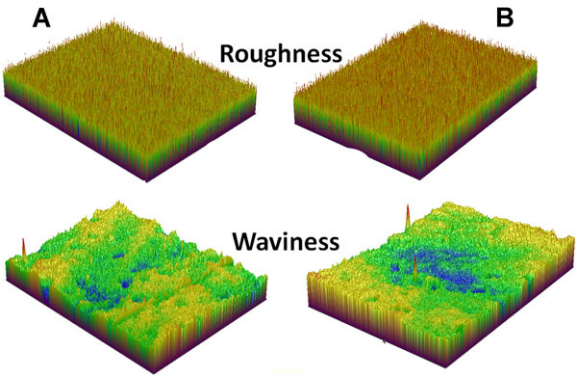

Figure 2. Roughness and waviness factors measured by optical interferometry of nonannealed surface (A) and annealed surface (B).

on them. Some of the consequences of these effects are the waviness and roughness.

To determine the impact of annealing on these features, optical interferometry measurements were performed. This technique allows us to analyze larger areas (micrometric scale) at nanometric distances. Figure 2 shows the differences between the arithmetic average of absolute values (Ra factors) in both roughness and waviness. The interferometry results show a decrease of four times on roughness of the annealed surface versus the untreated gold (0.04 nm versus 0.16 n, respectively). Large-scale measures allow us to say that annealing is not only a method for forming flat terraces of low roughness but also it masked glass support defects. This heating treatment helps to reduce the waviness of the glass substrate from 0.66 to 0.37 nm.

3.3 Voltammetry characterization of effective surface

To measure the effective conductive area in both type of nanostructured gold electrode surface, cyclic voltammetries were carried out in sulfuric acid, for measuring the experimental active area. For its mathematical calculation this formula reported in literature [25] was used;

$$Area = Q_{Au}{}^{*}(r_{Au}/r_{O2})^{2}/n\,Q^{0}$$

Where Q_{Au} is the area under the curve of the sulfuric acid reduction peak; $(r_{Au}/r_{O2})^2$ is the square of the atomic radius ratios between the gold substrate and the adsorbed oxygen; n is the number of electrons involved in oxygen oxidation and Q^0 is the reference charge for reduction of an oxide monolayer on polycrystalline gold. For this experiments Q^0 equal to 390 $\mu C\ cm^{-2}$ was considered [26].

Table 1 shows the results obtained with this electrochemical characterization. The variations of the real active area of gold after annealing and without annealing are compared with the geometric theoretic area of the electrode. From this results, it can be observed that the electrochemical roughness factor (ρ = experimental area/theoretical area) [27] in nonannealed surface is 2.4; while in the annealed electrode is only 1.2. Thus, the decrease of the roughness and the effective area after annealing treatment is nearly 50%, which approaches annealed surfaces to the theoretical value of ultraflat surfaces.

3.4 Surface coverage characterization with SPR

Once the nano-structuration of both studied substrates; pebble-type untreated gold and annealed flat terraces-type gold, has been characterized. The effect of the substrates roughness was studied in the performance of DNA biosensors.

SPR offers a deep understanding about the amount of biomolecules attached on the chip surface in each step of the biosensor set up. It should be point out that the heating treatment used in annealing for flattering the gold layer, directly impact on the SPR reproducibility, since the read out of this technique is intimately related with the thin metal layer on the SPR substrate. So, the metal heating protocol introduces a variable in all the treated substrates, as is appreciated in the higher standard deviation of the annealed substrates response.

The theoretical values of biomolecules surface coverage proposed in the table, were calculated taking into account shielding diameters of the MalPEG (1.17 nm) [28] as the basement of the bioreceptor immobilization and dsDNA diameter (2.55 nm) to consider the hybridized DNA in a perfect geometrical distribution of the biomolecules on the surface.

The differences observed on the roughness and effective area, are reflected in the adsorption rates of molecules in each type of substrate. The experimental values measured in the ultraflat annealed substrate shows a very similar bioreceptor surface coverage compared with the theoretical one. It was assumed that the theoretical values are calculated under a virtual flat surface, and the closer surface coverage values obtained on the annealed surface reveals that the treatment helps to achieve this goal, giving well-ordered and packed monolayers. On the other side, the grainy surface of the untreated gold has larger area of gold for the immobilization of bioreceptor interface.

The visible differences between the monolayer immobilization efficiency reflect structural changes of the gold surface (see Fig. 4.). The reorganization of the crystalline structure formed on flat terraces of gold, decreases the available places, also observed on the reduction of the effective area of the gold surface. For this reason, the bioreceptor molecules diminish its surface coverage on the annealed treated surfaces, comparing with nonannealed substrate that has higher roughness and so higher effective area and bioreceptor immobilization.

However, although more receptors site were deposited on the pebble-type surface, the amount of hybridized DNA molecules are lower comparing with the annealed flat chip, being the double of targets detected on the annealed one.

Table 1. Experimental and theoretical values of electrode areas characterized by CV

Surface coverage (Γ = molecules/mm^2)			
Monolayer	Theoretical values	Experimental values without annealing	Experimental values with annealing
Electrode area	0.567 (cm^2)	1.353 (cm^2)	0.661 (cm^2)
Bioreceptor	9.3×10^{11}	1.21×10^{12}	9.9×10^{11}
Target DNA	1.9×10^{11}	2.78×10^{10}	6.1×10^{10}
DNA hybridization efficiency	100%	14%	32.10%

Surface coverage (Γ) measured by SPR of bioreceptor immobilization and DNA target hybridization on annealed and nonannealed surfaces ($n = 3$).

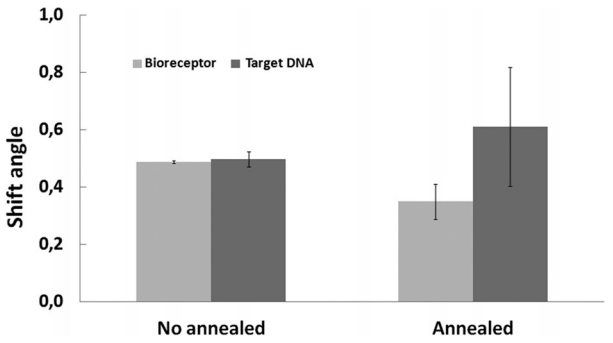

Figure 3. Angle shift in SPR characterization after bioreceptor immobilization and DNA target hybridization on annealed and untreated substrates.

Considering the theoretical value calculated for the covering of ds DNA molecules, in the case of ultraflat substrate was observed 32% of efficiency, while this percentage is reduce to 14% in the case of the grainy surface.

Dates show in Fig. 3 confirmed the varied distribution of biomolecules on the different nano-organized substrates.

Figure 3 shows the increase of angle due to the SPR chip covering. The change of refracted angle is measured under equal refractive index conditions on the chip before and after biomolecules incubation. So, the shift of angle is only due to the modification of the resonant oscillation of excited plasma with the adsorbed molecules on the gold chip. As it was commented in the previous table, higher adsorption of the bioreceptors is observed on the untreated surface. However, higher hybridization is detected on the ultraflat chip.

The new surface organization on the ultraflat substrates turns out in the formation of immobilization patterns that reduce both steric hindrances and electrostatic repulsion. The monolayer formation has been studied to form the thiol chains approximately $(\sqrt{3}x\ \sqrt{3})R30^\circ$ angle titled to the gold surface [29]. In a planar annealed surface the deposited molecules have the similar angle. However in the case of a pebble-type surface the monolayer follows the distortions of the flat surface. Thus, the well-ordered and organized distribution, in similar direction of the bioreceptors, in the planar configuration, contrast with the random orientation of the highly packed linking sites on the untreated substrate (Fig. 4). This chaotic distribution of the negatively charged bioreceptors hinders the entrance of the negatively charged DNA target.

Moreover, many of the features of the SAMs depend directly of the crystalline organization substrate where they are deposited. By changing this surface organization also changes the thermal stability and kinetics of chemisorptions of the head groups on gold and thus its distribution, covering, and angle with respect to the surface are different [30].

These small but important changes greatly enhance the hybridization efficiency, being the increase in more than twice in surface coverage DNA hybridization, although annealed substrate contains lower amount of bioreceptors.

3.5 Electrochemical DNA sensor characterization

The DNA target was amplified by PCR with a ferrocene-labeled primer, giving a 110-mer ferrocene labeled dsDNA. The redox reaction of the hybridized ferrocene molecule on the gold electrode surface was successfully detected by DPV.

From the electrochemical point of view, pebble-type electrodes have some drawbacks comparing with ultraflat substrates. The ions adsorbed on the grainy electrodes have a larger area for adsorption, and so higher capacitance effect [31]. In this way, the electron transfer from the ferrocene label to the electrode becomes more difficult, thus decreasing the signal obtained. Moreover, the charge redistribution between molecules in the ordered assembled interface has a beneficial effect on electron transport and charge transfer [32], helping in the transport of the electrons from the redox label to the electrode, and thus in the sensitivity of the electrochemical biosensor [31].The distance between oxidation and reduction peaks, the reversibility of a redox reaction, and reproducibility of electrochemical measurements, are also affected by the state and nature of the substrate [33].

Besides the fact that the flat electrodes have beneficial effects on the electrochemical read-out, the well-ordered distribution of the bioreceptors on annealed electrodes, as surface coverage characterization with SPR shown, demonstrate more efficient hybridization of the DNA target. The electrochemical characterization of the DNA biosensor on evaporated wrinkled gold electrodes and on annealed flat gold surfaces, shown higher hybridization efficiency in the sensor previously treated with annealing (see Fig. 5). In electrochemical sensors the improvement is much clearer than in optical detection, being more than twice in magnitude the current observed in the annealed system. These results

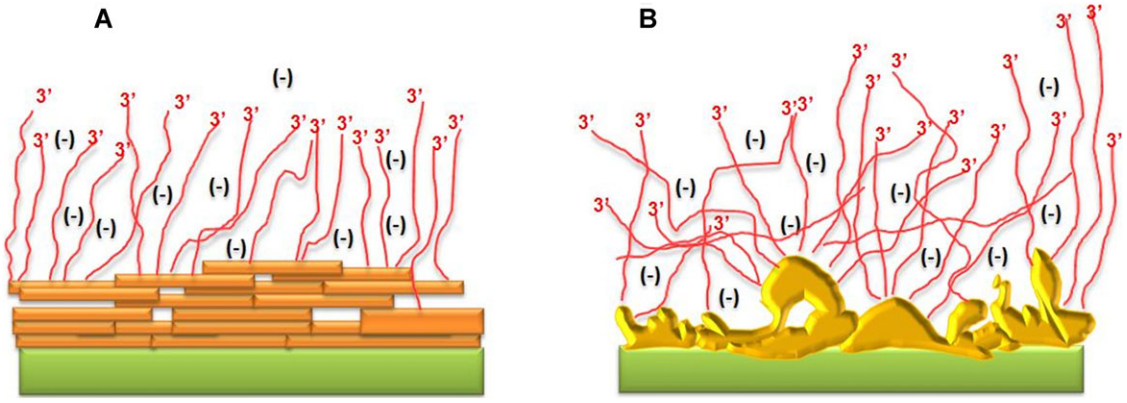

Figure 4. Schemes of different bioreceptor SAM distribution on ultraflat terraces of annealed (A) substrates and on rough not annealed (B) substrates. Note a well-ordered distribution of bioreceptors in annealed surface ($n = 3$).

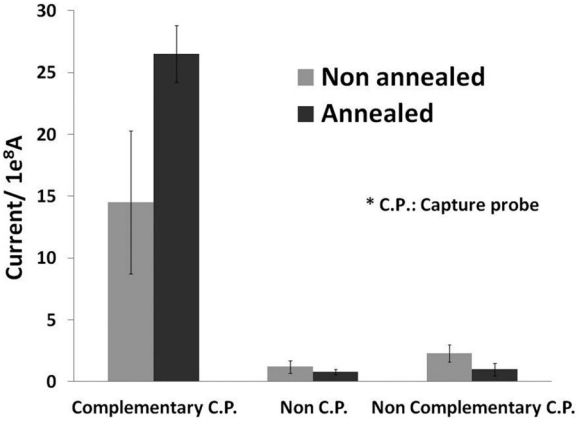

Figure 5. Current signal from DPV biosensor characterization on annealed and nonannealed substrates. DNA target biosensor response is plotted as complementary capture probe and the selectivity of the biosensor was tested with two controls, using a noncomplementary capture probe and without capture probe.

are due to the synergy effects on annealed substrates of both facts; a less steric hindrance for the target hybridization in a more ordered distribution of the bioreceptors, and easier transfer of the charge and less capacitance on the electrode.

The random distribution of the DNA captures on the nonannealed substrates brings a more unpredictable DNA arrangement and electron transfer and hence irreproducibility into the system, as is shown in Fig. 5. This irreproducible signal is represented by 38% of signal deviation in the untreated electrochemical DNA sensor, while only 8% was observed in the annealed biosensor.

Moreover, the disorganized interface on the sensor may give rise to the formation of uncovered areas on the substrate that attracts the undesired fouling of biomolecules. This fact is observed in the higher control currents detected in the untreated platform.

The increase of signal currents due to a more efficient hybridization event on annealed substrates is accompanied by a decrease of the controls signal. The synergy of both effects brings a better selectivity in the annealed platform. Although both systems demonstrates a clear differentiation between the selective signal from the complementary hybridization of the target and the unspecific signal from the controls, the more selective annealed sensor shows higher current signal difference of 2.56 nA, while only the half of this difference is observed on the untreated sensor (1.27 nA) (Fig. 5).

4 Concluding remarks

In summary, it was demonstrated that the annealing treatment on commercial gold evaporated substrates has a beneficial effect on the biosensor performance. The transition between the nanoparticulate substrate to the laminar-annealed surface has deep consequences over the biomolecules distribution and interaction and so in the sensitivity of the sensor. The heating treatment causes the molecular rearrangement of the gold, forming ultraflat terraces. The pebble-type untreated substrates, with higher surface area demonstrate broader bioreceptor coverage. However, the flat annealed surface favors improved and well-ordered bioreceptors patterns with its subsequent lower steric hindrance for the hybridization of the DNA target. The organization more homogeneous of the monolayers in annealed substrates results in a high quality monolayers and sensors. Moreover, an ordered charged bioreceptors interface facilitates the transfer of electrons from the redox label to the electrode and reduce the capacitance effects. This involves improvements in both the hybridization efficiency and electrochemical reading, making the annealing a powerful tool in the optimization of biosensors interfaces. An optimum standard treatment before the formation of SAMs is essential for developing efficient biosensing platforms.

This work was funded by the project OLIGOCODES from the Spanish Ministry of Economy and Competitiveness MAT2012-38573-C02. The Nanobioengineering group has support from the Commission for Universities and Research of the Department

of Innovation, Universities, and Enterprise of the Generalitat de Catalunya (2014 SGR 1442). CIBER-BBN is an initiative funded by the VI National R&D&i Plan 2008–2011, Iniciativa Ingenio 2010, Consolider Program, CIBER Actions and financed by the Instituto de Salud Carlos III with assistance from the European Regional Development Fund.

The authors have declared no conflict of interest.

5 References

[1] Ariga, K., Hill, J. P., Lee, M. V., Vinu, A., Charvet, R., Acharya, S., *Sci. Technol. Adv. Mater.* 2008, *9*, 014109 (96pp). doi:10.1088/1468-6996/9/1/014109.

[2] Satija, J.,Sai V. V. R., Mukherji, S., *J. Mater. Chem.* 2011, *21*, 14367–14386.

[3] Almeida, I., Cascalheira, A. C., Vilana, A. S., *Electrochimistry* 2010, Acta *55*, 8686–8695.

[4] Zhang, X., Guo, Q., Cui, D., *Sensors* 2009, *9*, 1033–1053.

[5] Simpson-Stroot, J. M., Kearns, E. A., Stroot, P. G., Magaña, S., Lim D. V., *J. Microbiol. Methods* 2008, *72*, 29–37.

[6] Walsh, M. K., Wang, X., Weimer, B. C., *J. Biochem. Biophys. Methods* 2001, *47*, 221–231.

[7] Brecht, A., Gauglitz, G., *Biosen. Bioelectronics* 1995, *10*, 923–936.

[8] Grieshaber, D., MacKenzie, R., Vörös, J., Reimhult, E., *Sensors* 2008, *8*, 1400–1458.

[9] Huang, E., Satjapipat, M., Han, S., Zhou, F., *Langmuir* 2001, *17*, 1215–1224.

[10] Gong, P., Lee, C. Y., Gamble, L. J., Castner, D. G., Grainger, D. W., *Anal. Chem.* 2006, *78*, 3326–3334.

[11] Kolská, Z., Říha, J., Hnatowicz, V., Svorcík, V., *Materials Lett.* 2010, *64*, 1160–1162.

[12] Goss, C. A., Charych, D. H., Majda, M., *Anal. Chem.* 1991, *63*, 85–88.

[13] Golan, Y., Margulis, L., Rubinstein, I., *Surface Science* 1992, *264*, 312–326.

[14] Janícek, P., Kolská, Z., Mistrík, J., Siegel, J., Sutta, P., Svorcik, V., Worsch, P., *Appl. Phys. A* 2011, *102*, 605–610.

[15] Vericat, C., Vela, M. E., Benitez, G., Martin Gago, J. A., Torrelles, X., Salvarezza, R. C., *J. Phys. Condens. Matter* 2006, *18*, R867–R900.

[16] Hugall, J., Finnemore, A. S., Baumberg, J., Steiner, U., Mahajan, S., *Langmuir* 2012, *28*, 1347–1350.

[17] Mohn, F., Gross,L., Moll, N., Meyer, G., *Nat. Nanotechnol.* 2012, *7*, 227–231.

[18] Siegel, J., Krajcar, R., Kolská, Z., Hnatowicz, V., Švorčík. *V., Nanoscale Res. Lett.* 2011, *6*, 588.

[19] Feng, G., Niu, T., You, X., Wan, Z., Kong, Q., Bi, S., *Analyst* 2011, *136*, 5058–5063.

[20] Yu, F., *Ph.D. Thesis, Johannes Gutenberg-Universität, Mainz, Germany* 2004.

[21] Stenberg, E., Persson, B., Roos, H.; Urbaniczky, C., *J. Colloid Interface Sci.* 1991, *143*, 513–526.

[22] Koga, K., Ikeshoji, T., Sugawara, K., *Phys. Rev. Lett.* 2004, *92*, 115507–115510.

[23] De Los Santos, V. L., Lee, D., Seo, J., Leon, F. L., Bustamante, D. A., Suzuki, S., Majima, Y., Mitrelias, T., Ionescu, A., Barnes, C. H. W., *Surface Sci.* 2009, *603*, 2978–2985.

[24] Svorcík, V., Kvítek, O., Říha, J., Kolská, Z., Siegel, J., *Vacuum* 2012, *86*, 729–732.

[25] Quiroz, M. A., Morales, U., Meas, Y., Slagado, L., *Revista Mexicana de Física* 1993, *39* 722–737.

[26] Zuliani, C., Walsh, D. A., Keyes, T. E., Forster, R. J., *Anal. Chem.* 2010, *82*, 7135–7140.

[27] Jarzqbek, G., Borkowska, Z., *Electrochimica Acta* 1997, *42*, 2915–2918.

[28] Wolf, H., Ringsdorf, H., Delamarche, E., Takami, T., Kang, H., Michel, B., Gerber, Ch., Jaschke, M., Butt, H-J., Bamberg, E., *J. Phys. Chem.* 1995, *99*, 7102–7107

[29] Dubois, L. H.; Nuzzo, R. G., *Annu. Rev. Phys. Chem.* 1992, *43*, 437.

[30] Love, J. C., Estroff, L. A., Kriebel, J. k., Nuzzo, R. G., Whitesides, G. M., *Chem. Rev.* 2005, *105*, 1103−1169.

[31] Hoogvliet, J. C., Dijksma, M., Kamp, B., van Bennekom, W. P., *Anal. Chem.* 2000, *72*, 2016–2021.

[32] Leopold, M. C., Bowden, E., *Langmuir* 2002, *18*, 2239–2245.

[33] Engelkes, V. B., Beebe, J. M., Frisbie, C. D. *J. Am. Chem. Soc.* 2004, *126*, 14287–14296

